www.serd.ait.ac.th/reric

An Experimental and Numerical Study on Pressure Drop Coefficient of Ball Valves

A. Ozdamar*[1], K. Turgut Gursel*, Y. Pekbey*, and B. Celikag

Abstract – *In this study, a computational method to predict steady and single-phase flows inside a pipe joined to a ball valve has been examined. Flow computations have been performed using the finite volumes method. To this aim, governing equations for continuity and momentum are first integrated over a control volume, and then the resultant algebraic equations are numerically solved. Results obtained indicate the change of the fluid velocity and pressure fluctuation depending on longitudinal direction inside the pipe. In addition to the computational study, results from the experimental study carried out under the same conditions were obtained to compare with the results of the computational method. Thus, the experimental study does not only confirm sufficient sensitivity of the results obtained from the computational model, but it also indicates a relation between the ball valve opening and the pressure drop coefficient. Thus, the proposed computational model may be used as a tool to design better and efficient installation systems with different ball valves.*

Keywords – Ball valve, computational fluid dynamics, experimental fluid dynamics, finite volumes method, minor loss, pressure drop coefficient, turbulence model.

1. INTRODUCTION

Minor loss values for ball valves indicate averaged losses given by various manufacturers. However, it is well known that there is an uncertainty up to ± 50 percent [1], [2]. Due to the complex geometry of ball valves, manufacturers' design details influence almost all minor losses of valves in different flows, which exactly can be determined only experimentally.

Steady and single-phase flows are encountered in several engineering applications from the simple flow inside a pipe to the flow of a river. Several studies have been performed in the past to analyze the characteristics of such flows. Recent developments in computational fluid dynamics (CFD) enabled researchers to simulate almost all kinds of problems that can occur in real situations as presented in [3]. In study of Larachi *et al.* [4], a different engineering application of CFD method in exploring bed pressure drop of single-phase gas flow in towers is available. Erdal [5] studied several parameters affecting turbulent mixing and fully developed flow conditioning downstream of a plate by using CFD tools. Halupovich et al. [6], calculated the steady two-dimensional viscous supersonic turbulent flow by using a CFD code and the two-equation *k-ε* turbulence model for the turbulent flow simulation in investigating turbulent supersonic flow. Erdal and Andersson [7] executed a full pipe simulation to primarily investigate various grid effects, coordinate arrangements and turbulence models in order to predict more accurate flow values through an orifice in two-dimensional axisymmetric flow. Similar studies regarding turbulent and laminar gas flows, which use the CFD method, were executed in [8]-[10]. However, in the corresponding literature, comparisons regarding minor loss values of ball valves obtained numerically and experimentally could not be found.

Steady and single-phase flows occurring as internal flows particularly are of great importance. The flow inside a pipe that is joined to a ball valve is an example of internal free, steady and turbulent single-phase flow. The objective of the present study was to develop a CFD model that can predict the steady free flows inside a pipe controlled by a ball valve, in order to obtain the pressure drop coefficient (ζ) by means of the CFD method [11]. Further, these numerical results were compared to those of the experiments carried out under the same conditions. In agreement of these results, this model could be used for designing installation systems with new types of ball valves without executing expensive experiments, and uncontrolled pressure drop that causes blockages, noise and energy losses in piping systems could be reduced with the developed model, which is usually the general aim in engineering applications.

2. EXPERIMENTAL DETERMINATION OF THE MINOR LOSS COEFFICIENT OF A BALL VALVE

The measured minor loss coefficient is usually defined as a ratio of the head loss along the setup to the head velocity of the fluid [1]:

$$\zeta = \frac{2gh}{u^2} \tag{1}$$

Where;

$$h = \frac{\Delta p}{(\rho g)} \quad \text{and} \tag{2}$$

Δp : Difference between inlet and outlet pressure.

* Mechanical Engineering Department, Faculty of Engineering, Ege University, 35100 Bornova – Izmir, Turkey.

1 Corresponding author;
Tel./Fax: 00-90-232-3888562.
E-mail: aydogan.ozdamar@ege.edu.tr

In this study, a steady-state turbulent air flow with an inlet temperature of 293 K and an inlet pressure of 2500 Pa has been considered. To avoid disturbances before and after the opening due to the present valve, the inlet and outlet straight pipe sections were joined to the valve as shown in Figure 1.

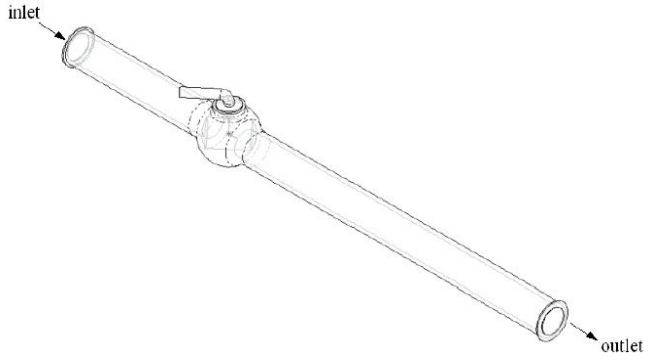

Fig. 1. Ball valve joined to straight pipe

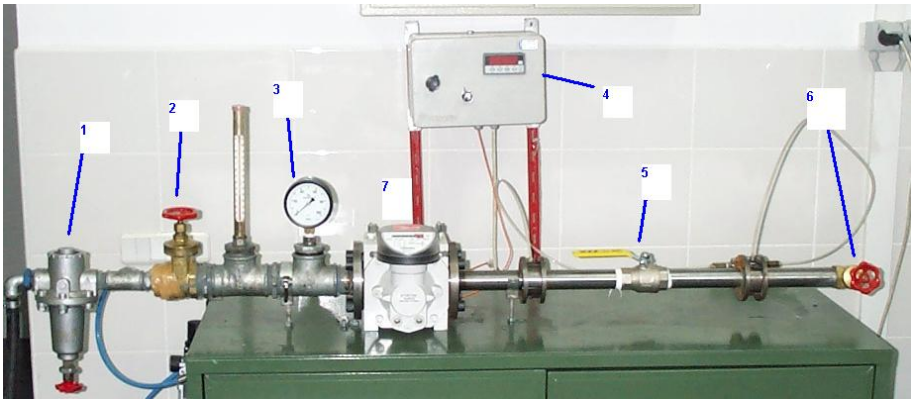

Fig. 2. Experiment facility

As seen in Figure 2, the system consists of a ball valve of DN 32 (5), regulation valves at the inlet and outlet sections (1,2,6), a flow meter measuring the flow rate of air passing through the system (7), a manometer measuring inlet pressure (3) and an electronic panel measuring pressure difference between the inlet and the outlet sections (4). The compressed air flows into the system through the plug valve (2). The inlet pressure of the air is set to 2500 Pa by the pressure regulator as shown in the manometer (3). When the ball valve (5) is at "fully-opened" position, outlet pressure is set to 2400 Pa by means of the valve (6). The difference between inlet and outlet pressure can be observed on the digital panel (4) as 100 Pa during the experiment process. Under these circumstances, the volume flow rate of the air is measured per minute. When the handle of the ball valve is turned towards its fully-opened position, change in the flow rate is also measured.

First, the aim of the experiment was to determine the response of the system when the increase of pressure difference reaches 100 Pa for the fully-opened position of the ball valve. The valve inlet pressure was gradually increased up to 3500 Pa, whereas the outlet pressure was kept constant at 2400 Pa, and volumetric flow rates (Q) were measured by a flow meter.

In the next steps, the handle of the ball valve was turned towards its closed position 10° once again, after volumetric flow rates (Q) were measured. The minor loss coefficients were determined by Equation 1 with measured pressure differences Δp and respective velocities that were calculated from the volumetric flow rates.

3. NUMERICAL DETERMINATION OF THE MINOR LOSS COEFFICIENT OF A BALL VALVE

In principle, two different classes of numeric solution methods exist, which complement each other in practical application. In the first class, one proceeds from a solution assumption for a sought-after variable already before the execution of the approximation calculation. This variable is approximated in form of a finite series, in which the series' elements after a certain number are to be neglected according to the needed accuracy. For instance, Galerkin's method belongs to this class of methods with the special advantage that the individual assumption function accurately fulfills the boundary conditions of the flow problem examined. The disadvantage of these otherwise exact solution methods lies in the fact that in some cases no suitable assumption functions can be found. Hence, for the mentioned flow problems, such numeric solution methods are generally used, which directly solve the partial differential equations approximately after discretisation of the integration area without any assumption functions selected beforehand. The finite volumes method belongs to this numeric solution one [12].

CFD codes contain different numeric solution methods of partial differential equations of fluid flows such as the Navier-Stokes and Euler equations. For

solving these differential equations, the finite volumes method is developed that it satisfies the conservation equations (continuity, momentum and energy) discretized over each volume element in the computational domain with better accuracy.

Governing Equations

The cornerstone of computational fluid dynamics is the fundamental governing equations of fluid dynamics; namely the continuity, momentum and energy equations. In the present study, the Eddy-Viscosity Model was applied for solving the Reynolds Averaged Navier-Stokes equations (RANS), and Reynolds stresses were modeled by using an Eddy-Viscosity μ_t [13]. The continuity equation and the unsteady incompressible RANS equation are respectively written as follows:

$$\frac{\partial U_i}{\partial x_i} = 0 \tag{3}$$

$$\rho U_k \frac{\partial U_i}{\partial x_k} = -\frac{\partial p}{\partial x_i} + \mu \frac{\partial^2 U_i}{\partial x_j \partial x_j} + \frac{\partial R_{ij}}{\partial x_j} \tag{4}$$

In Equations 3 and 4, mean velocity components U_i and Reynolds stresses R_{ij} are given as:

$$U_i(\vec{x},t) = u_i(\vec{x},t) - u_i'(\vec{x},t) \tag{5}$$

$$R_{ij} = -\rho \overline{u_i' u_j'} = \mu_t \left[\frac{\partial U_i}{\partial x_j} + \frac{\partial U_j}{\partial x_i} \right] \tag{6}$$

In Equation 5, u_i and u_i' denote fluid velocity and velocity fluctuation, respectively. The Reynolds stresses in Equation 4 obtained from Equation 6 include additional unknowns introduced by the averaging procedure; hence they must be added in order to complete the equations. In Equation 6, μ_t is calculated in Standard k-ε Model that is defined as:

$$\mu_t = 0.09 \rho \frac{k^2}{\varepsilon} \tag{7}$$

In Equation 7, k and ε respectively denote turbulent kinetic energy and the dissipation rate.

Representative fluid velocities are obtained by solving the Equations 3 and 4 through the domain in FLUENT 6.0 with respect to boundary conditions, which are explained in the following sections [14], [15].

Solution Methodology in Fluent 6.0

i. Grid generation

In the present study, a two-dimensional geometrical system with sizes of 476 mm x Ø36 mm is considered for numerical analysis of the problem as shown in Figure 3. The modeled system possesses the same external dimensions as the testing facility of the commercial ball valve. A computational grid of hex/wedge elements is generated using the preprocessor of the commercial software "GAMBIT" as given in Figure 4.

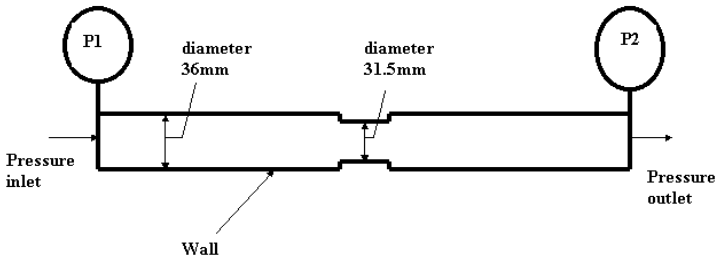

Fig. 3. Geometrical sizes of the experiment facility

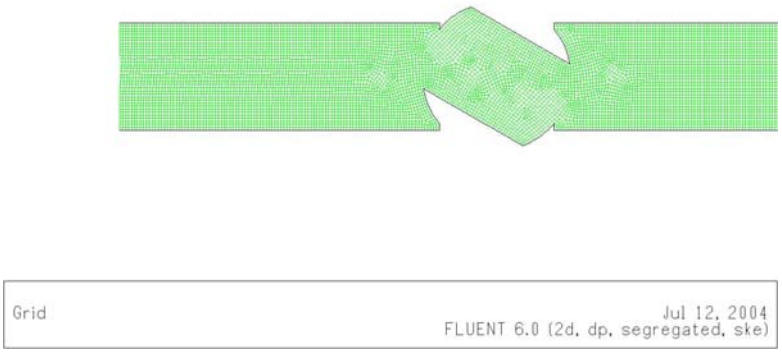

Fig. 4. Typical grid used in CFD analysis

As seen in Figure 3, the inlet and outlet diameters of the pipe are 36 mm, and the diameter of the ball valve, which permits the passage of the fluid through the pipe, is 31.5 mm. The pressure values p_1 and p_2 correspond to the manometers that were mounted onto the inlet and outlet sections of the pipe.

ii. Boundary Conditions

In this CFD analysis, the various physical boundary conditions were applied as given in Table 1. The computational and experimental studies were carried out under pressure difference of 100 Pa between the inlet and outlet sections (Table 2).

Table 1. Applied boundary conditions

Nr	Physical Boundary Conditions	Computational Boundary Conditions
1	Inlet	Pressure Inlet
2	Axis	Axisymmetric
3	Fluid	Air
4	Outlet	Pressure Outlet

Table 2. Boundary conditions values used

Nr	Parameter	Value
1	Inlet Gauge Total Pressure	100 Pa
2	Outlet Gauge Total Pressure	0 Pa
3	Density	1.225 kg/m^3

iii. Solution Procedure

Governing differential equations are integrated over each control volume, which yields a set of algebraic equations that are numerically solved. The pressure and velocity are obtained by using the approach algorithm of *k-ε* standard turbulence modeling by Spalding, since the flows are turbulent at Re>2,300 and Re>20,000 in internal and external flows, respectively, which also apply in FLUENT software. Calculations in this study were performed with using implicit viscous model solver as post-processor.

After obtaining the results of numerical analysis, velocity magnitude changes and static pressure changes through the pipe system for ball angle of opening $\theta = 90°$, 50°, 20° are shown in Figures 5, 7, and 9 and Figures 6, 8, and 10, respectively.

4. RESULTS AND DISCUSSION

In this study, a computational method to predict steady and single-phase flows inside a pipe joined to a ball valve has been investigated. Additionally, results obtained from the experiment performed under the same conditions have been compared to the results of the computational method.

In the computational analysis of the present study, it is assumed that the fluid inside the pipe is continuous and incompressible due to the low *Mach*-number, although it is air. Table 3 shows the velocities in experiment and simulation for comparison.

The outlet velocities obtained in the experiment are slightly lower than those in simulation. Similarly, pressure drop coefficients of the simulation model are slightly lower than those of the experimental model. Figure 11 shows pressure drop coefficient relation depending on the opening angle of the ball valve. It can be clearly seen that the results obtained from the experiment and CFD analysis exactly agree with each other especially in ball angles of opening between 90° and 30°. Besides, the agreement of the results between 30° and 0° is satisfactory. While the ball angle decreases, the pressure drop coefficient ζ increases rapidly, this reaches up to infinite value at the angle from 13° and up to the fully-closed position. In addition, while the pressure difference between the inlet and outlet sections increases, the pressure drop coefficient ζ remains constant.

Table 3. Change of the pressure drop vs. the outlet velocity

D_p [Pa]	Outlet velocity in experiment [m/s]	Outlet velocity in CFD [m/s]
100	10.81	12.01
200	15.26	16.95
300	18.68	20.75
400	21.55	23.94
500	23.95	26.61
600	26.26	29.172
700	28.36	31.51
800	30.32	33.69
900	32.27	35.85
1000	34.06	37.84

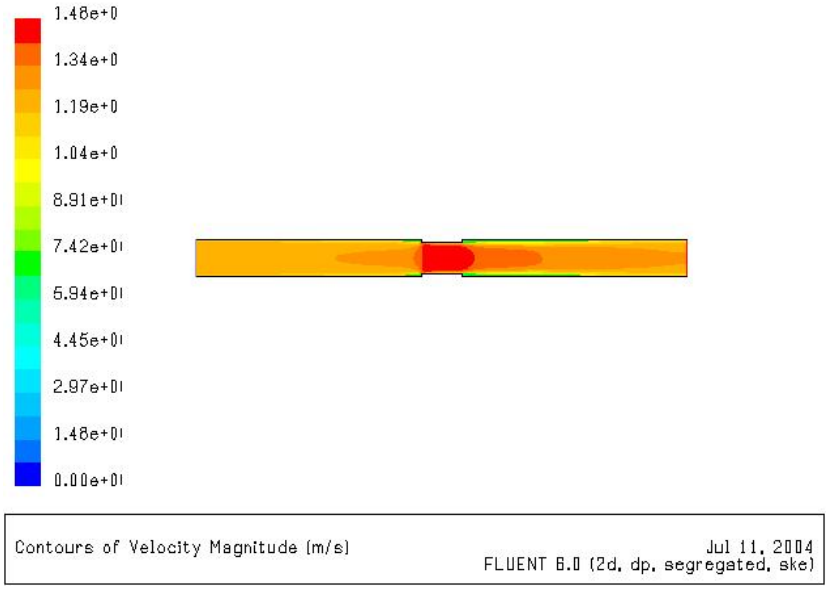

Fig. 5. Axial velocity magnitude change through the pipe (ball angle of opening θ =90^0)

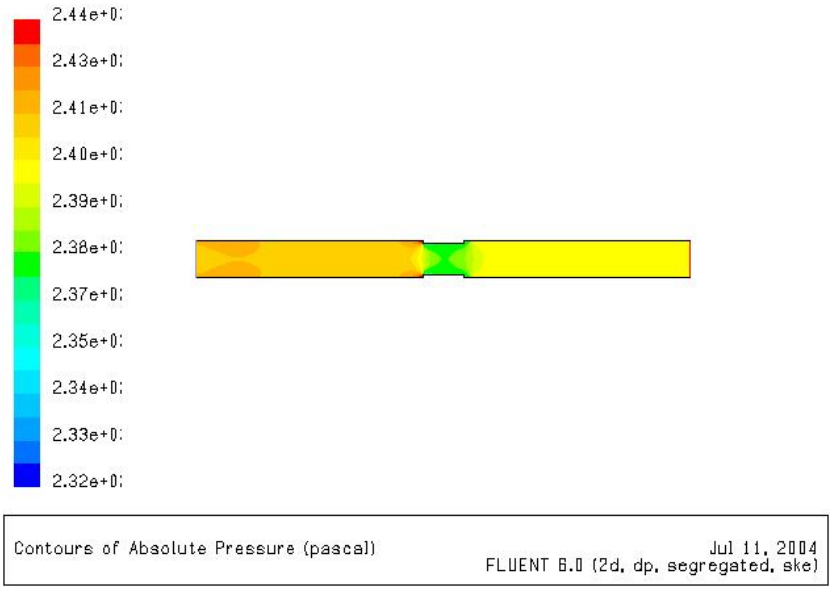

Fig. 6. Static pressure change through the pipe (ball angle of opening θ =90°)

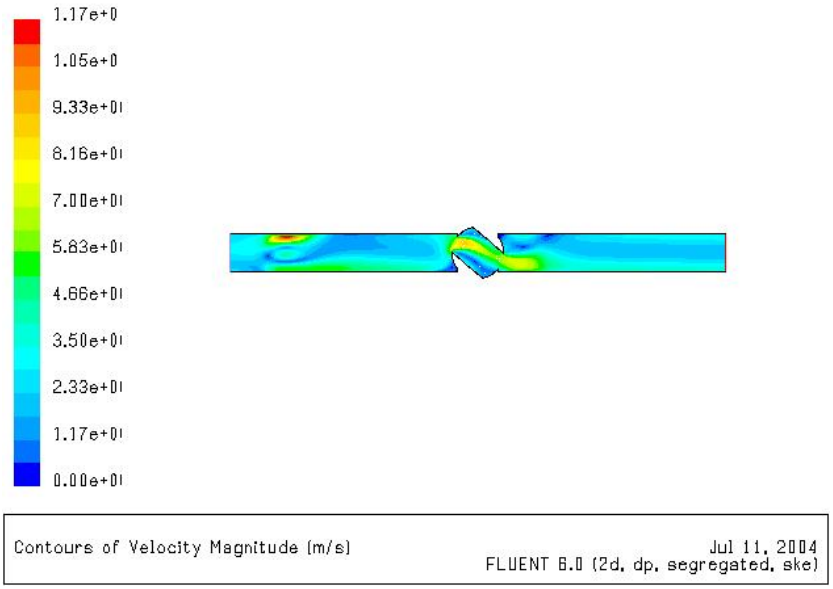

Fig. 7. Axial velocity magnitude change through the pipe (ball angle of opening θ =50°)

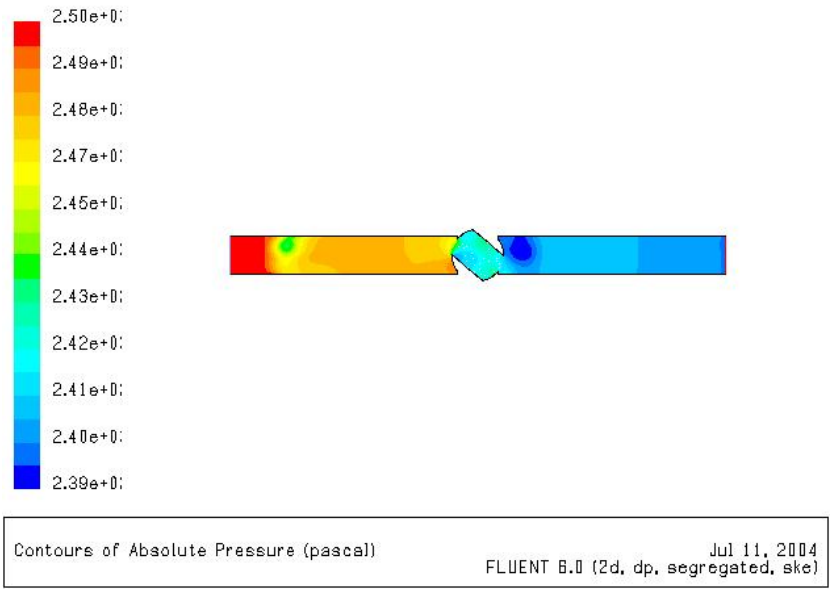

Fig. 8. Static pressure change through the pipe (ball angle of opening θ =50°)

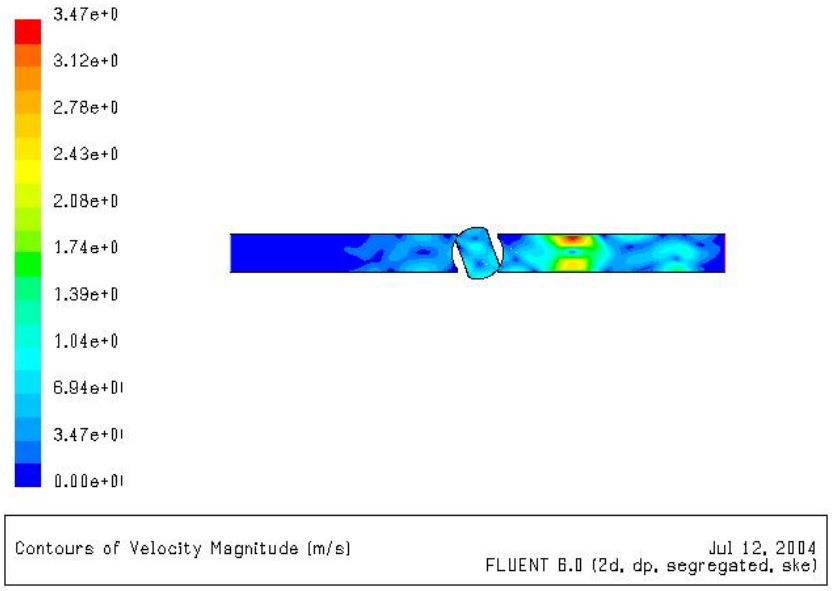

Fig. 9. Axial velocity magnitude change through the pipe (ball angle of opening θ=20°)

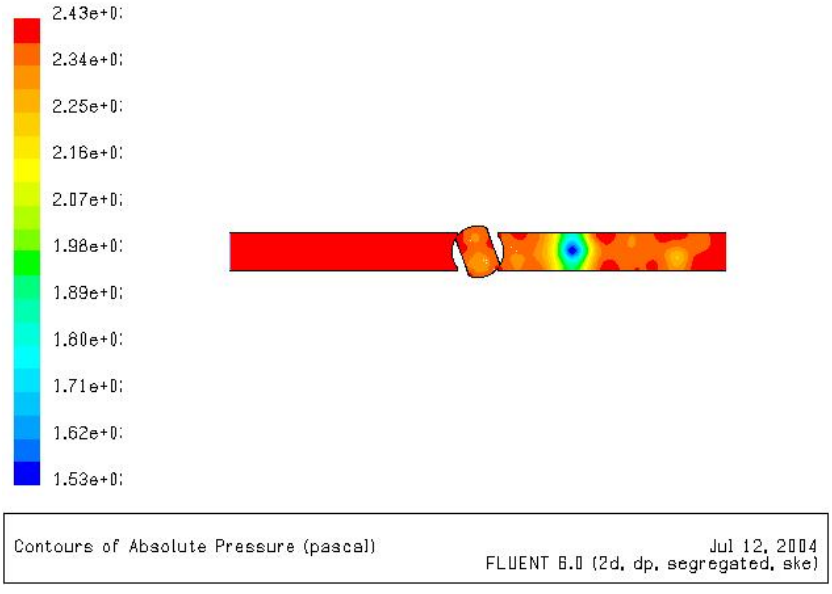

Fig. 10. Static pressure change through the pipe (ball angle of opening θ=20°)

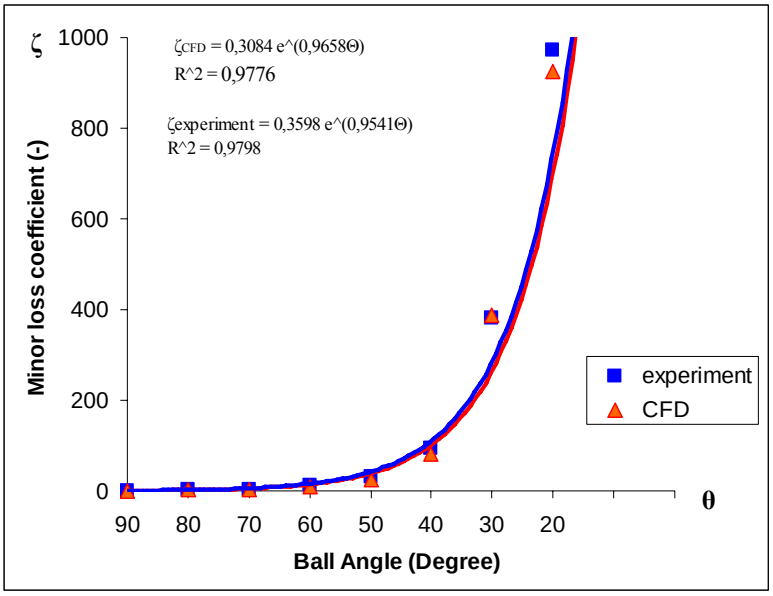

Fig. 11. Relation of pressure drop coefficient ζ vs. ball angle of opening in comparison of experiment and CFD analysis

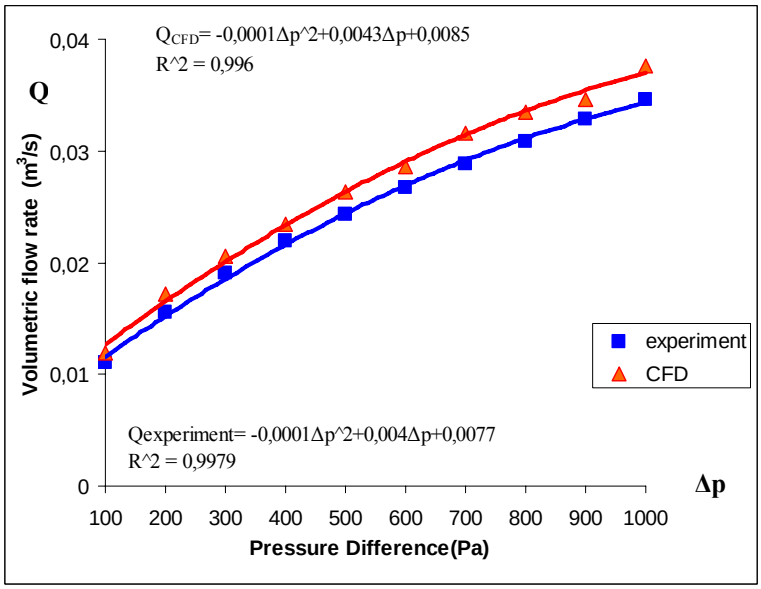

Fig. 12. Relation of pressure drop vs. flow rate

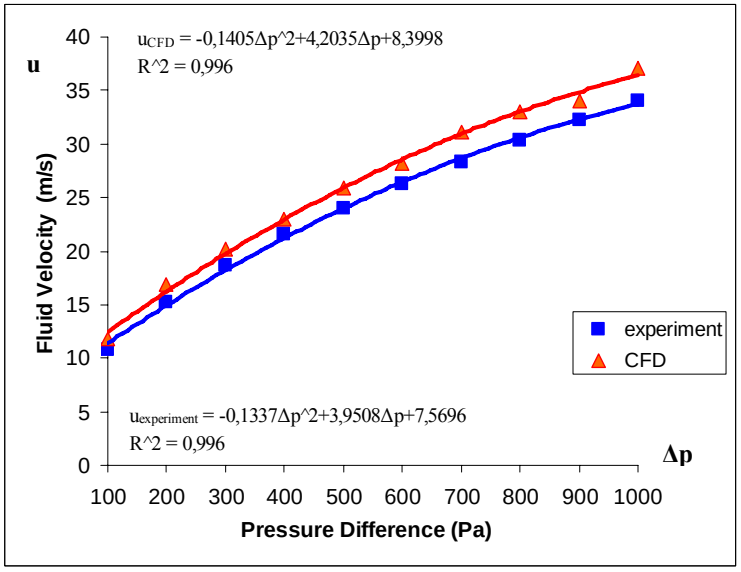

Fig. 13. Relation of pressure drop vs. axial velocity

Figure 12 shows the relation between the volumetric flow rate and the pressure drop. The results exhibit that the pressure difference between the inlet and the outlet sections increases with the increasing volumetric flow rate. Additionally, Figure 12 represents a satisfactory agreement between the CFD analysis results and those of the experiment as in Figure 13 that similarly exhibits the change of the increasing inlet pressure versus the axial velocity.

In other words, after 13° of opening angle, the pressure drop coefficient decreases down to 1200. When the ball valve is turned towards its fully-opened position, the pressure drop coefficient reaches its minimal value, namely "zero".

Generally, the experimental velocities were determined lower than simulation results. This is due to the constructional reasons such as fittings that it was normally impossible to measure the pressure values exactly on points where numerical calculations were carried out. Additionally measuring accuracy partially was derogated by any losses.

5. CONCLUSION

The pressure drop coefficient values of other valve types are much higher than those of the ball valve, which is the main reason why the ball valves are used when low-pressure drop is especially required. The results obtained in the experiment and CFD analysis indicate that the computational model adopted can be used as a tool to design better and efficient installation systems with different ball valves subjected to similar conditions such as those of this experiment.

Additionally, pressure drops in piping systems cause blockages, noise and energy losses, which have to be reduced as much as possible. By using the fully-opened ball valve, by minimizing the pipe length and maximizing the inside pipe diameter, and by avoiding unnecessary valves, filters and bends along a pipe system, users may obtain triple savings in energy consumption, pipe and fitting costs.

NOMENCLATURE

Symbols	Explanation
G	Acceleration of gravity
h	Head
k	Turbulent kinetic energy
p	Pressure
Q	Volumetric flow rate
R_{ij}	Reynolds stresses
U_i	Mean velocity
u_i	Fluid velocity
u_i'	Velocity fluctuation
v	Velocity component in direction of radial axis
Δp	Difference between inlet and outlet pressure
θ	Ball angle
ε	Turbulent dissipation rate
μ_t	Eddy viscosity
ζ	Pressure drop coefficient
P	Density

REFERENCES

[1] White, F.M. 2004. *Fluid Mechanics*, McGraw-Hill, 5. Ed., New York.

[2] Skousen, P.L. 1988. *Valve Handbook*, McGraw-Hill, New York.

[3] Bhaskaran, R., and Collins, L. 2003 Introduction to CFD Basics. Lecture notes accessed at http://courses.cit.cornell.edu/fluent/cfd/

[4] Larachi, F., Petre, C.F., Iliuta, I., and Grandjean, B. 2003. Tailoring the pressure drop of structured packings through CFD simulations. *Chemical Engineering and Processing* 42, 535-541.

[5] Erdal, A. 1997. A numerical investigation of different parameters that affect the performance of a flow conditioner. *Flow. Meas. Instrum.* 8/2, 93-102.

[6] Halupovich, Y., Natan, B., Rom, J. 1999. Numerical solution of the turbulent supersonic flow over a backward facing step. *Fluid Dynamics Research* 24, 251-273.

[7] Erdal, A., and Andersson, H.I. 1997. Numerical aspects of flow computation through orifices. *Flow. Meas. Instrum*. 8/1, 27-37.

[8] Fu, W.S., and Ger, J.S. 1999. A concise method for determining a valve flow coefficient of a valve under compressible gas flow. *Experimental Thermal and Fluid Science* 18, 307-313.

[9] Amati, G., Succi, S. and Benzi, R. 1997. Turbulent channel flow simulations using a coarse-grained extension of the lattice Boltzmann method. *Fluid Dynamics Research* 19, 289-302.

[10] Makarytchev, S.V., Langrish, T.A.G., and Fletcher, D.F.. 2002. CFD analysis of spinning cone columns: Prediction of unsteady gas flow and pressure drop in a dry column. *Chemical Engineering Journal* 87, 301-311.

[11] Ozdamar, A., Gursel, K.T., Pekbey, Y., and Celikag, B. 2004. A preliminary study on pressure drop coefficient of ball valves. Ege University Scientific Research Project Report (02/MUH/024), Izmir, Turkey (In Turkish).

[12] Oertel, H., and Böhle, M. 2002. *Stroemungsmechanik, 2nd Edition.* Vieweg Verlag, Braunschweig.

[13] Paciorri, R., Bonfiglioli, A., Di Mascio, A., and Favini, B. 2005. RANS simulations of a junction flow. *International Journal of Computational Fluid Dynamics*, Vol. 19, No. 2, 179–189.

[14] Fluent Software Training Notebook, "Why model turbulence", TRN-00-002, Fluent Inc., 2002.

[15] Fluent Software Training Notebook, "Two equation model", TRN-00-002, Fluent Inc., 2002.